Geofísica Internacional (2001), Vol. 40, Num. 1, pp. 31-41

Coast effect in magnetotelluric soundings over the Yucatán peninsula, Mexico

Omar Delgado-Rodríguez[1,2], Jaime Urrutia-Fucugauchi[1], Jorge A. Arzate[3] and Oscar Campos-Enríquez[1]

[1] *Departamento de Geomagnetismo y Exploración, Instituto de Geofísica, UNAM, México, D.F., México*

[2] *Instituto de Geofísica y Astronomía. CITMA, La Habana, Cuba*

[3] *Unidad de Investigación en Ciencias de la Tierra, UNAM-Campus Juriquilla, Juriquilla, Qro., México*

Received: May 2, 2000; accepted: December 13, 2000.

RESUMEN

A partir de la modelación sintética de la península de Yucatán se pudo establecer que el efecto de costa sobre las mediciones magnetotelúricas realizadas en la región de impacto de Chicxulub es despreciable.

La plataforma marina que circunda a la península produce un moderado efecto de costa en un rango de períodos (T= 10 a 1000 s) que no se corresponde con los períodos (T= 1 a 10 s) que definen la anomalía conductora en las curvas de resistividad eléctrica aparentes observadas en las 22 estaciones MT.

Estos resultados le ofrecen una alta confiabilidad a los obtenidos del levantamiento MT, por lo que se proponen otras áreas, igualmente confiables, para ejecutar nuevas mediciones MT.

PALABRAS CLAVE: Sondeo magnetotelúrico, modelación 3-D, efecto de costa, cráter de Chicxulub, península de Yucatán.

ABSTRACT

Three-dimensional synthetic modeling of magnetotelluric sounding data of the Yucatán peninsula suggests that the coast effect on the magnetotelluric measurements carried out over the Chicxulub impact region is negligible. The marine platform surrounding the Yucatán peninsula yields a moderate coast effect in a period range T= 10 to 1000 s, outside of the period range associated wih the conductivity anomaly of the crater (T= 1 to 10 s). These results provide a framework for the interpretation of MT soundings previously obtained in the Chicxulub crater and define other areas for future MT surveys in the Yucatán peninsula.

KEY WORDS: Magnetotelluric sounding, 3-D modeling, coast effect, Chicxulub crater, Yucatán peninsula.

INTRODUCTION

Discovery of the Chicxulub crater on the Yucatán peninsula, Mexico (Figure 1), with an age at the Cretaceous-Tertiary boundary (65 million years b.p.) supports the hypothesis of an extraterrestrial impact (Alvarez *et al*., 1980).

During the past decade, geophysical studies have been carried out at the Chicxulub impact structure, including gravity and magnetic information (e. g., Hildebrand *et al*., 1991, 1998; Sharpton *et al*., 1993; Pilkington *et al*., 1994; Espíndola *et al*., 1995). Different models (e.g., four rings basin, simple ring, with diameter of 300 km, 180 km diameter, with central structural high with twin peaks) have been proposed.

Recently, models have been based on marine seismic reflection profiles (e. g., Morgan *et al*., 1997). In addition, lithological and geomorphological information was compiled in order to document the subsurface stratigraphy (e. g., Connors *et al*., 1996; Urrutia-Fucugauchi *et al*., 1996).

Magnetotelluric (MT) soundings provide information on the conductivity structure of the Yucatán peninsula (Campos-Enríquez *et al*., 1997). Twenty-two MT soundings were measured along two radial AA' and BB' profiles (Figure 2). The survey showed the presence of fracture zones in the lower crust, and no evidence of a mantle uplift. Delgado-Rodríguez *et al*. (2000) carried out a 1-D inversion of profile BB' using the Bostick (Goldberg and Rotstein, 1982) and Occam algorithms (Constable *et al*., 1987). They provided support of a 1-D representation and they found a diameter of approximately 200 km for the crater. Arzate *et al*. (2000) carried out a 2-D inversion of both profiles, and established a diameter of the structure of around 195 km.

The peninsular environment raises the question of the dependence of the electromagnetic models on the coast effect (Dosso and Meng, 1992). This paper discusses the coast effect on the MT soundings performed over the Chicxulub impact structure.

COAST EFFECT

The coast effect in electromagnetic observations was described by Parkinson (1959) as a result of the influence of the high electric conductivity of sea water (Kellet *et al*., 1991).

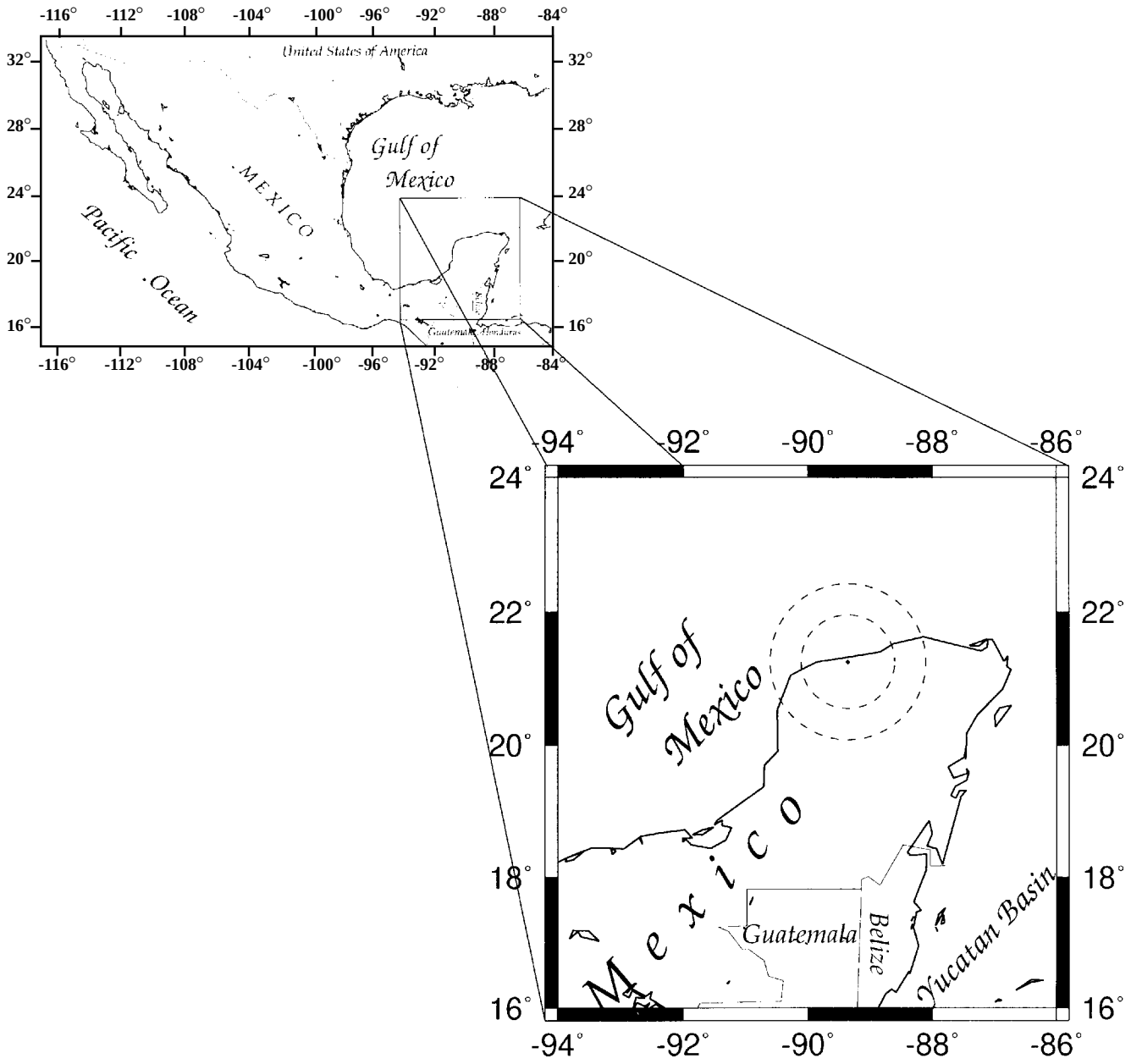

Fig. 1. Study area. Two of the proposed diameters of the structure are indicated with the town of Progreso in the center.

The influence of a highly conductive body may affect geomagnetic measurements in a way that suggests a spurious presence of a conductive stratum in the interpretation of curves $\rho(\omega)$ and $\phi(\omega)$. In addition, it can mask the real effect of an anomalous conductive body, possibly associated with the Chicxulub impact crater.

Laboratory models of the coast effect have been constructed, which simulate conditions in different situations (Meng *et al*., 1979; Nienaber *et al*., 1979; Hebert *et al*., 1983; Chen *et al*., 1990). Dosso and Meng (1992) empirically determined some mathematical relations that estimate the effect for continental conditions and for islands.

The coast effect is measured by means of the relation B_z/B_{yn}. between the induced vertical magnetic field B_z and normal magnetic field B_{yn}. A value of 1nT was assigned to B_{yz}. The ratio B_z/B_{yn} depends on the distance from the coastline, it reaches its highest value at the coastline and decreases seaward as well as inland.

The influence of the coast effect can be evaluated when the distance of the coastline Y_r is long enough, so that the relation $B_z/B_{yn} = 0.2$. Otherwise, the coast effect is very difficult to calculate. B_z/B_{yn} increases with increasing ocean depth and decreases with the increase of period T. Dosso and Meng (1992) published sets of curves for different types of

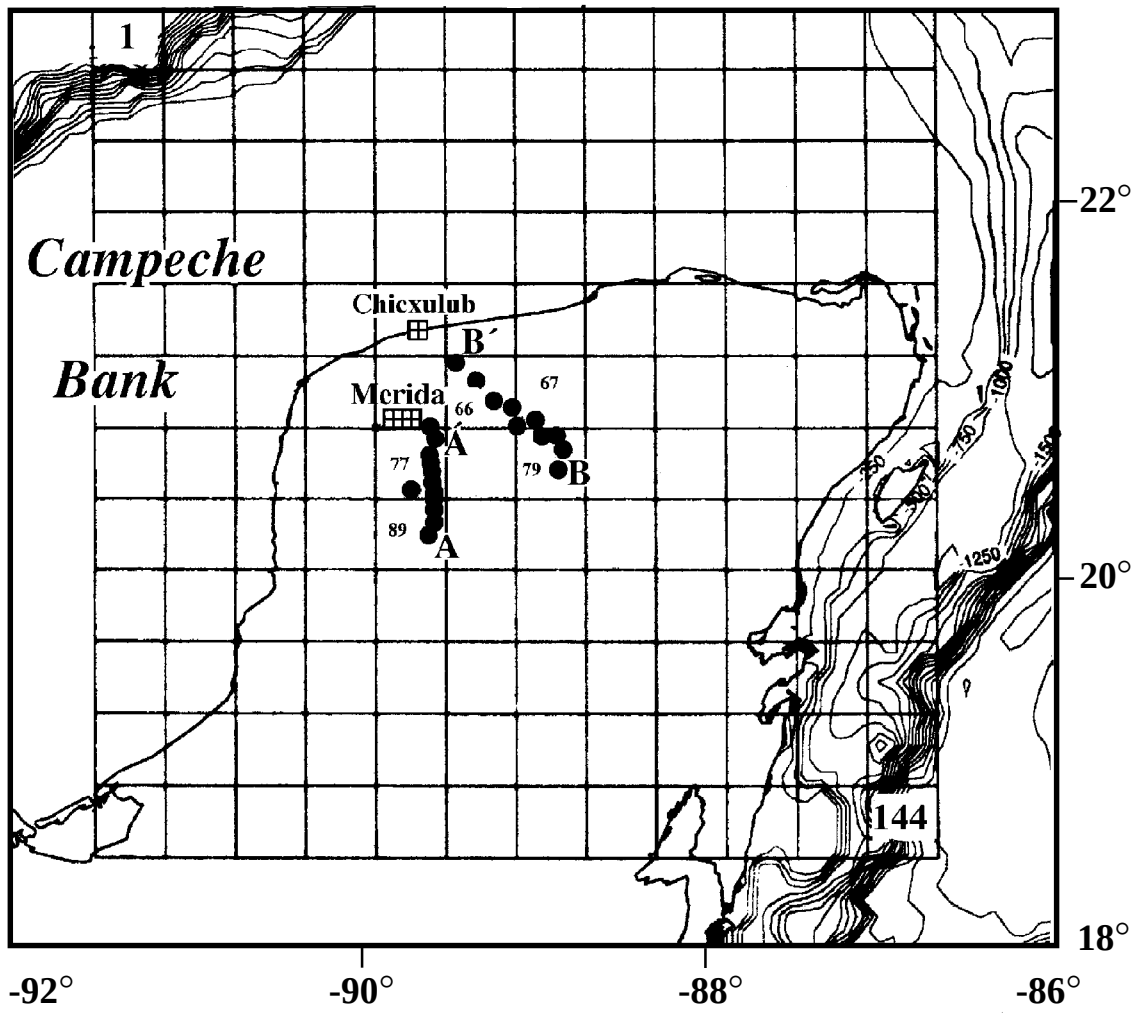

Fig. 2. Plan view of the synthetic 3-D model.

islands, providing the distance at which $B_z/B_{yn} = 0.2$ is reached as well as the distance Yr.

3-D MODELING

A direct 3-D modeling scheme is used by means of the program 3DMT (Park, 1985).

The procedure consists of designing a network of blocks that contain the information on the distribution of the electric resistivities of the medium. In the design of the model three factors are considered:

1.- The thickness of any inhomogeneous layer should be smaller than the nominal depth (skin depth). Calculation of the skin depth uses the lowest electric resistivity and the highest frequency considered in the calculations. The thickness of any inhomogeneous layers should be less than 20% of the nominal calculated depth (Park, 1985).

We find a minimum skin depth of 350 m for model 3B (Figure 3B); thus a cell thickness not larger than 70 m should be selected. We use a value of 50 m which factors integrally into 2 km and yields a total of 50 layers of 50 m thickness. For the model 3A (Figure 3A) the thickness is smaller.

2.- Lateral extension of the blocks should not be greater than the Minimal Adjustment Distance (AD). The AD parameter constitutes a nominal horizontal distance capable of influencing the inhomogeneities perturbing the 1-D solution in each block.

In order to calculate AD, average resistivities larger than 100 ohm-m present in the medium are considered by calculating the value of effective electric resistivity (Park, 1985).

$$\rho_{eff} = \frac{\sum \rho_i \Delta Z_i}{\Delta Z_{eff}}, \qquad (1)$$

$$\Delta Z_{eff} = \sum \Delta Z_i \,, \qquad (2)$$

where ρ_i is the electric resistivity larger than 100 ohm-m in layer *i*, and

ΔZ_i is the thickness in km of layer i.

Thus, the *AD* distance is calculated by

$$AD = \sqrt{\frac{\Delta Z_{block} * \rho_{eff} * \Delta Z_{eff}}{\rho_{block}{}^4}} \,, \qquad (3)$$

where ρ_{block} is the electric resistivity of the inhomogeneous block in ohm-m, and

ΔZ_{block} is the thickness in km of the inhomogeneous block.

In our case ρ_{eff} = 8921.6 ohm-m, ΔZ_{eff} = 51 km, ρ_{block} = 500 ohm-m, ΔZ_{block} = 2 km and *AD* = 42.6 km. Thus it is possible to use a lateral dimension 40 x 40 km for each cell.

3.- Selection of the electric resistivity values for each layer, is subject to the solution of the two previous steps.

With these constraints, a 3-D resistivity model for the Yucatán peninsula and its margins is constructed. The magnetic and electric field components are calculated individually for each block. Next the values of the impedance tensor Z(ω) are determined as well the values of $\rho_{axy}(\omega)$, $\phi_{xy}(\omega)$ and $\rho_{ayx}(\omega)$, $\phi_{yx}(\omega)$ for each block and all periods.

The Yucatán peninsula model is constructed by one inhomogeneous superficial layer, 2 km thick, that represents the carbonated rocks (ρ = 500 ohm-m) covering the impact structure, and a marine platform around the peninsula (Figure 3) The effect of the sea on MT measurements was modeled independently with a model including the marine platform (Figure 3A), and another model based on a 1-D approximation of the platform (Figure 3B).

Comparing both models should bring out the effect of a conductive sea on the apparent resistivity values for several periods.

The model is represented by a network of 12 x 12 cells with a size of 40 x 40 km each (Figure 2).

At depth, it includes two layers with ρ = 5000 ohm-m and ρ = 10 000 ohm-m, respectively. Their thicknesses are 11 and 40 km (Figure 3).

The 3-D modeling of both models was carried out for periods of 0.001, 0.004, 0.01, 0.04, 0.1, 0.4, 1, 4, 10, 40, 100, 400 and 1000 s.

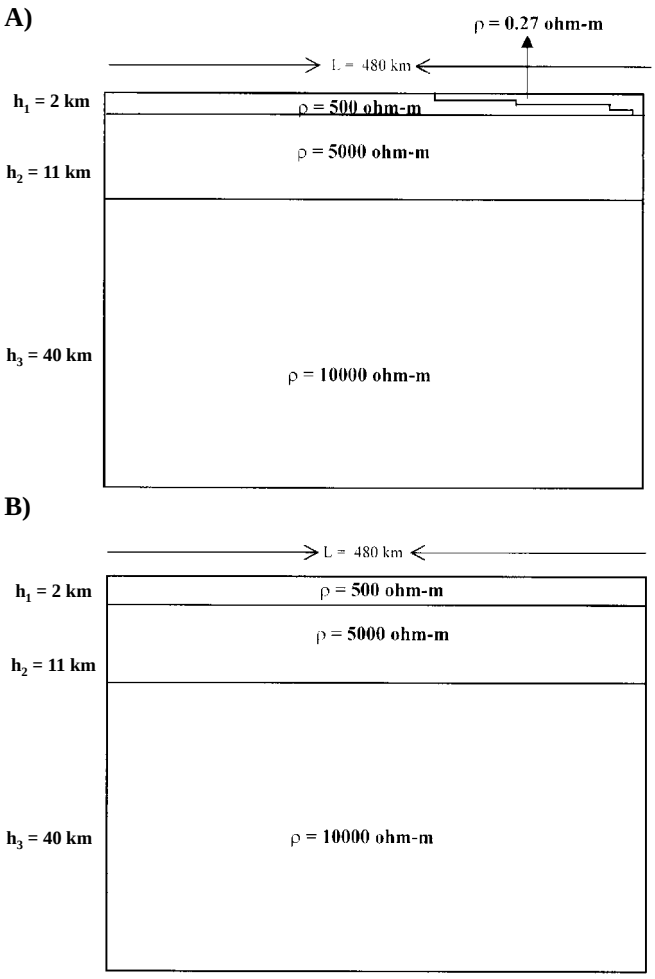

Fig. 3. Schematic sections of the models used in the 3-D synthetic modeling of the Yucatán peninsula. A) Model with marine platform, B) 1-D model.

RESULTS AND DISCUSSION

Figure 2 shows the 22 MT soundings distributed along two profiles (AA' and BB') contained in the cells 77 and 89 for profile AA', and 66, 67 and 79 for the profile BB'. Figure 4 shows the calculated apparent resistivity curves corresponding to cells 77 and 89, which include the profile AA'.

In both cells, the difference between the model that includes the marine platform and the 1-D model is small. This reflects the minor influence of the conductive sea on the profile. The most significant differences are observed in the period range of 10 to 100 s.

For the case of the profile BB', the curves corresponding to the cells 66, 67 and 79 (Figure 5) show a similar phenomenon, with some differences in the period range of 20 to 1000 s. The period of T = 100 s seems to be the most representative of these differences.

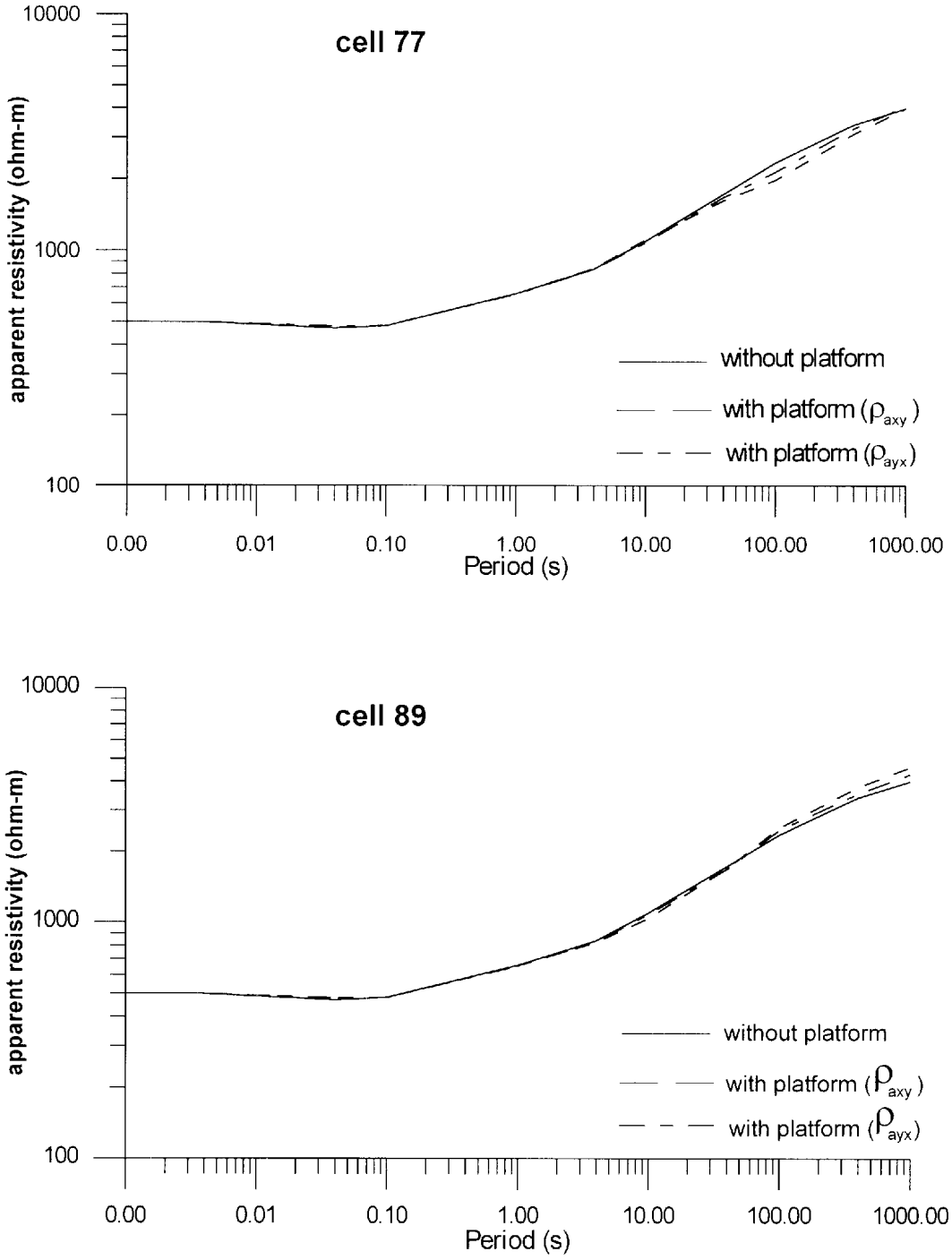

Fig. 4. Comparison of the apparent electric resistivity curves calculated from models 1-D and with marine platform. Cells 77 and 89 include the profile AA'.

In conclusion, the coast effect can only be seen in the range of periods of 10 to 1000 s, while the conductivity anomaly associated with the filling of the crater is present mainly in the periods of 0.01 to 10 s (Figure 6).

The apparent resistivity differences between 1-D model and the model with a marine platform were calculated for T=100 s for each cell over the peninsula of Yucatán and the surrounding marine platform. These differences are summarized for the *xy* mode (N-S) and the *yx* mode (E-W).

For the *xy* mode (Figure 7A) the difference is less than 10% in the area that includes most of the stations belonging to profiles AA' and BB'. The rest of the stations shows dif-

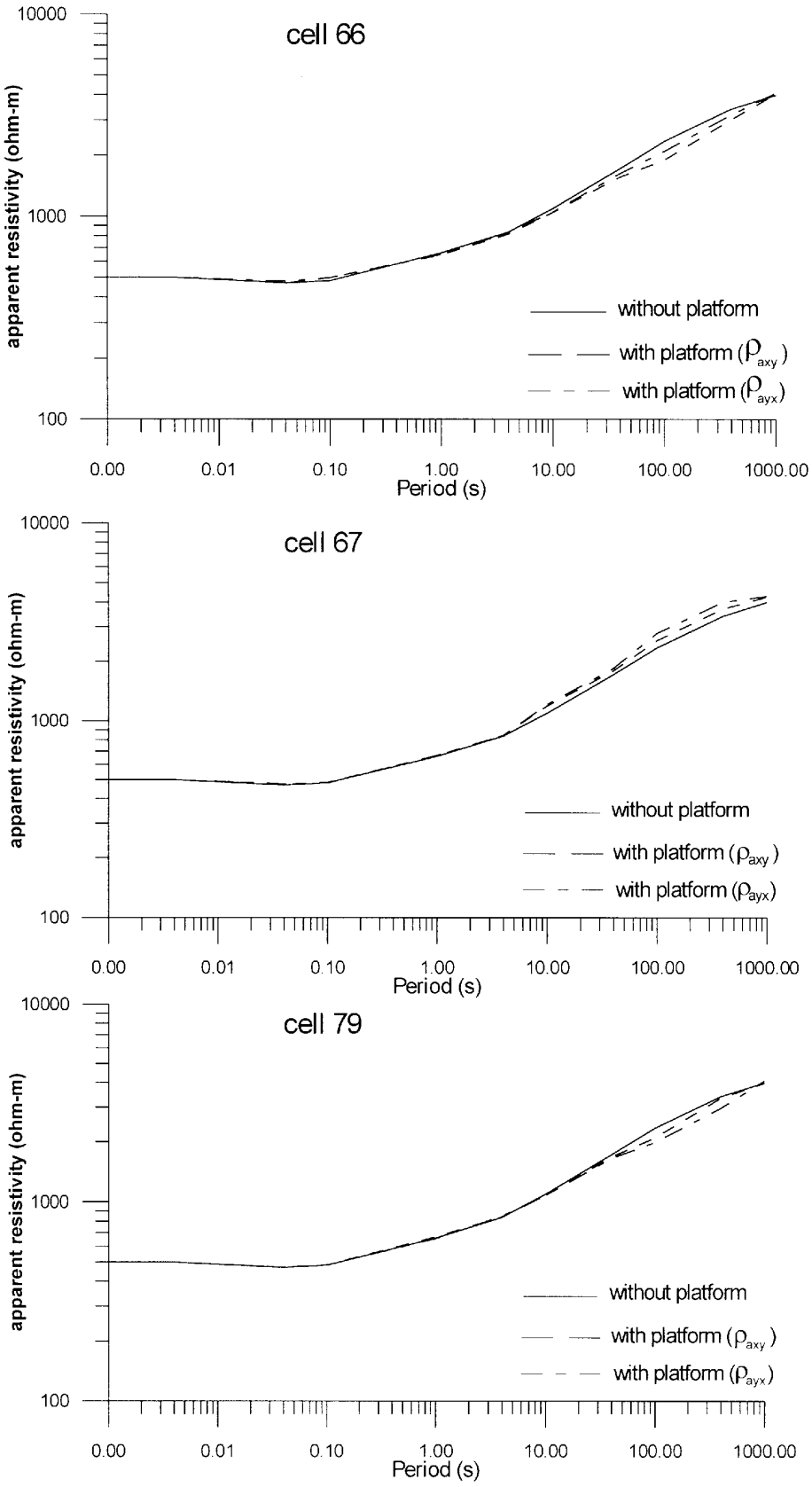

Fig. 5. Comparison of the apparent electric resistivity curves calculated from models 1-D and with marine platform. Cells 66, 67 and 79 include the profile BB'.

ferences of around 10%. The greatest differences in the peninsula are found in the area where the marine platform vanishes and the margin of the Yucatán basin appears. The increase in water depth near the coast increases the coast effect. Thus the curves of apparent resistivity calculated with the model of Figure 3A show a significant conductive anomaly at T = 100 s, that include a large negative difference in percentage.

The induction arrows were determined at each of the MT stations for T = 100 s (Figure 7A). In general, the induction magnitude is less than 0.4, being lower toward the interior of the cenote ring.

Northern Yucatán shows a higher density of fractures outside the cenote ring than inside it (Pilkington *et al.*, 1994). This explains the difficult to establish a predominant way in the discontinuous conductivity body.

In the case of profile BB', three stations (15, 16 and 17) have magnitudes and strikes that match with the location of the cenote ring.

The cenote ring coincides with the larger horizontal gravity gradient, as well as with a topographical depression (Connors *et al.*, 1996). The cenote ring is the surface expres-

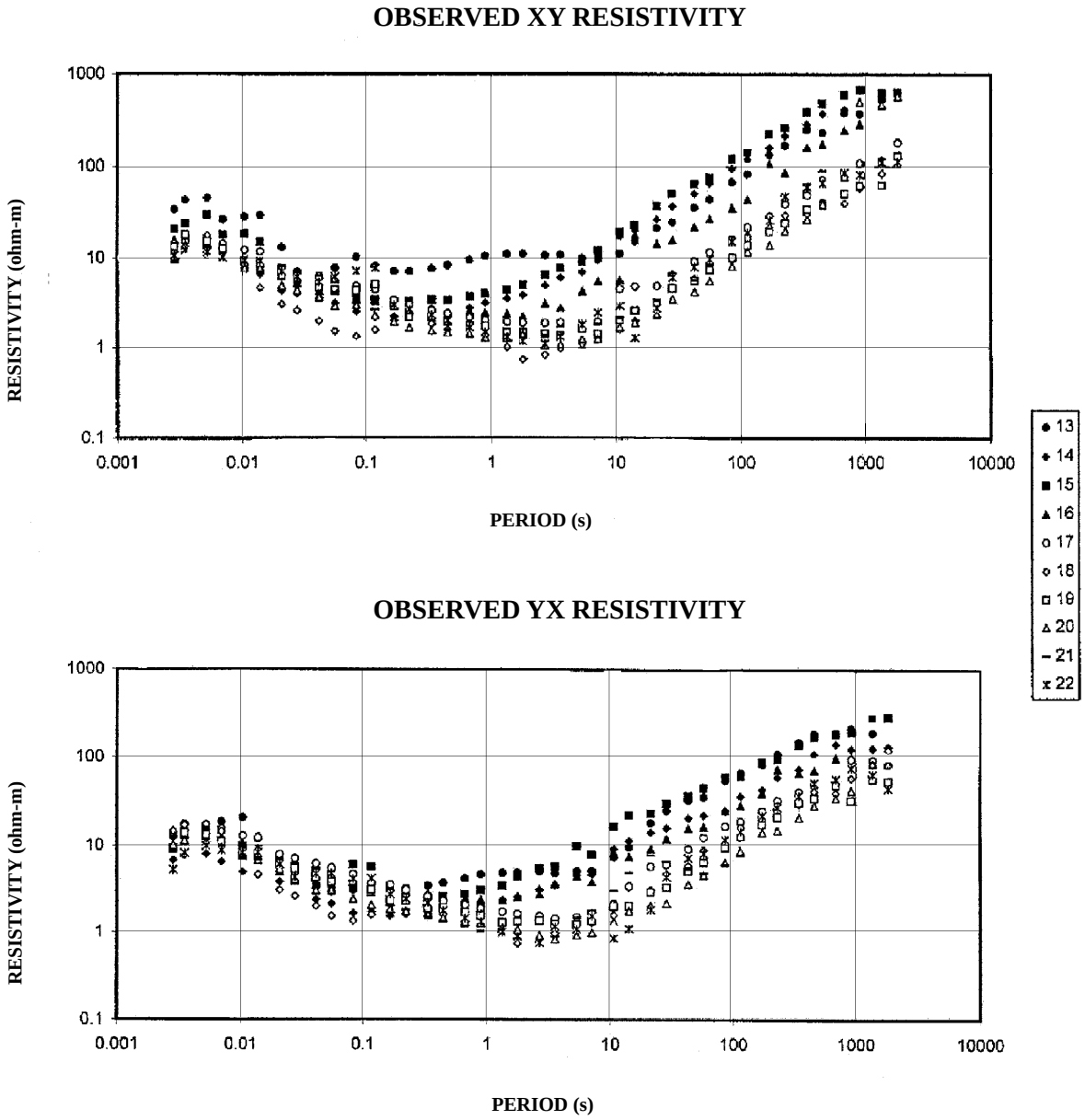

Fig. 6. Observed apparent resistivities curves for the profile BB'.

A)

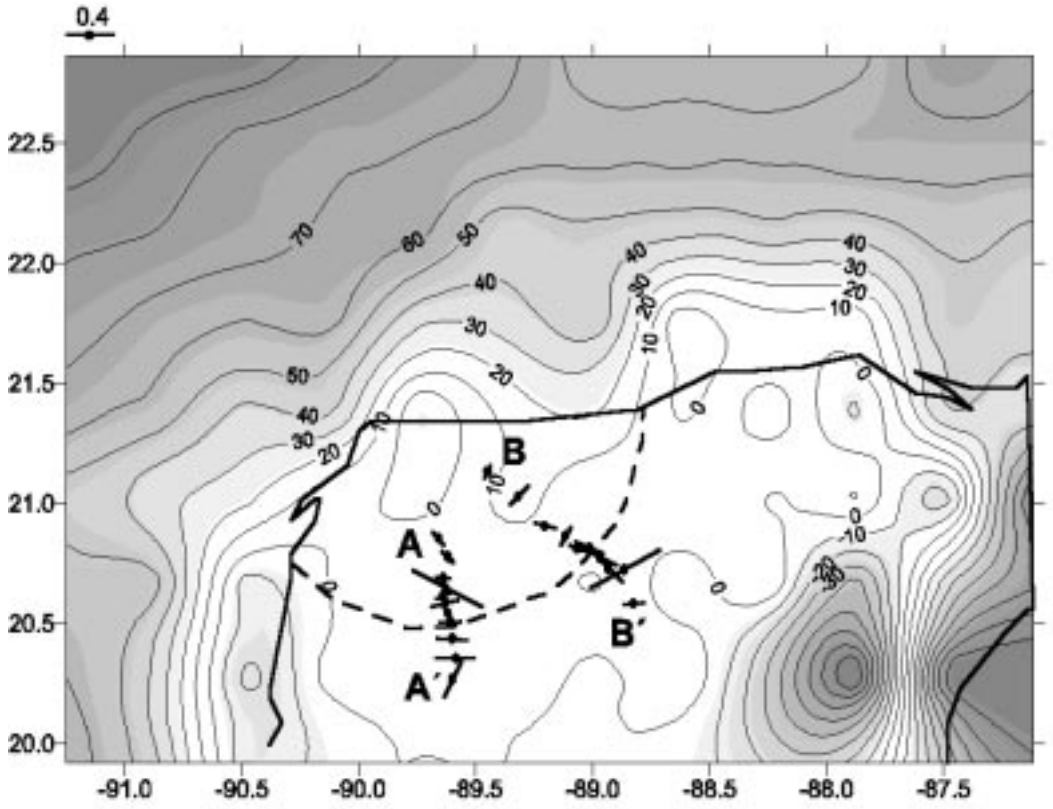

B)

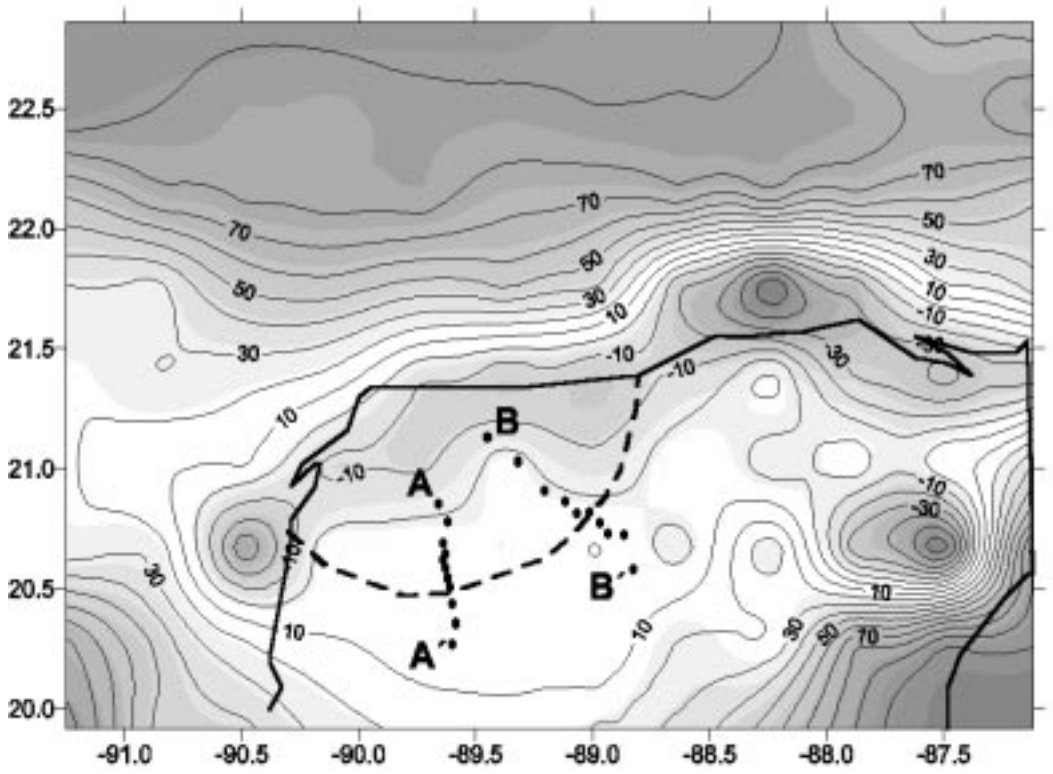

Fig. 7. Maps of coast effect for T = 100 s. A) *xy* mode. The induction arrows are represented at each station for T = 100 s; B) *yx* mode. The values on the map are given in percent. The approximate location of cenote ring is represented in dash line.

sion of a zone of concentric faults associated with the crater structure.

This is less evident in the profile AA', which runs along the gravity depression that extends for more than 100 km south of the cenote ring. Thus there is a more complex structure in the zone where the profile AA' is located, and therefore an undefined predominant direction is expected in the lateral heterogeneous discontinuities.

For the *yx* mode (Figure 7B) the results are similar to those in the *xy* mode (Figure 7A). The percentile differences are similar for the profiles AA' and BB', where the coast effect is important they cover a larger area toward the east of Yucatán peninsula. The TM mode is more affected by the coast effect (Vozoff, 1972). In this mode the current lines are normal to the coastline. Our *yx* mode is the TM mode for the eastern and western coastlines of the peninsula, while the *xy* mode is the TM mode for the northern coastline.

The areas of maximum coast effect on the TM mode in Figure 7 are mapped in Figure 8, showing the area of the Yucatán peninsula where MT soundings at periods larger than 100 s should not be carried out. The area of maximum coast effect is shaded. The coast effect increases to the east and northeast of the Yucatán peninsula, because of the presence of the margin of the Yucatán basin. The rapid increase of water depth in the Yucatán basin causes the coast effect to increase for higher values of T.

However, in the frequency range of interest (T< 100 s), the coast effect should become still smaller (see Figures 4 and 5), as the smaller marked area nearest to the eastern coastline of the Yucatán peninsula suggests.

CONCLUSIONS

All MT stations are located in areas where the coast effect is very low. Our calculations define new suitable areas to carry out further MT measurements without significant coast effect, even for periods larger than 100 s.

The curves of apparent resistivity calculated from models of the Yucatán peninsula with a marine platform, and a simple 1-D resistivity model, were compared, and an insig-

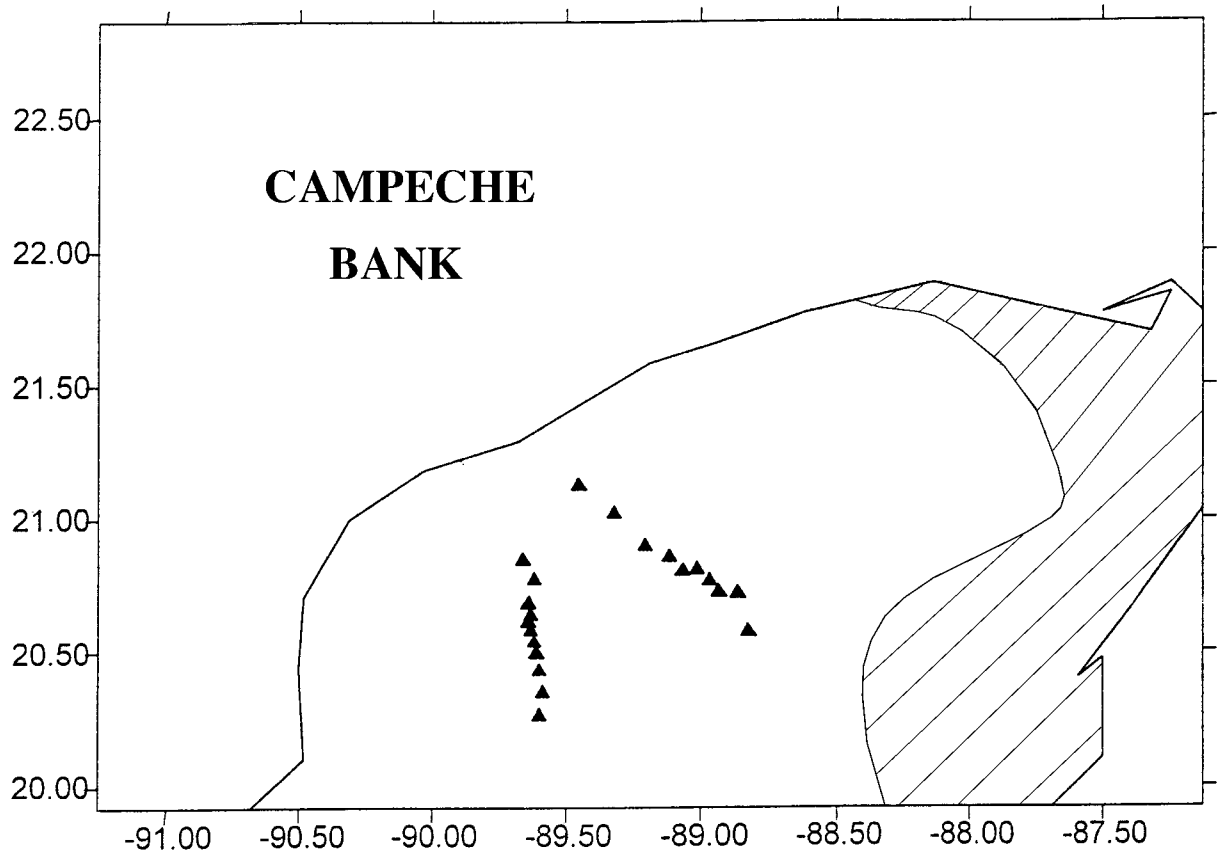

Fig. 8. Map of maximum coast effect for the period T = 100 s. The zones where the difference between the curves for both models is larger than 20% are shaded.

nificant effect of the sea on the MT soundings in the Chicxulub impact crater structure was observed.

A coast effect can only be appreciated in the range of periods of 10 to 1000 s. The anomaly associated with conductive filling of the crater is present mainly in the range of 0.01 to 10 s. The maximum coast effect for the area is found in the period T = 100 s.

A map of maximum coast effect for T= 100 s has been constructed. This map shows the influence of the margin of the Yucatán basin, which creates a zone of maximum coast effect in the eastern and northeastern end of the Yucatán peninsula.

We conclude that the coast effect on MT soundings in the Yucatán peninsula is negligible, and should have no significant effect on the interpretation of geoelectric models for Chicxulub crater.

Reliable MT soundings may be carried out everywhere, except in the marked areas with high coast effect, when MT observations for periods larger than 100 s are required.

ACKNOWLEDGMENTS

We acknowledge useful comments by three reviewers. Partial economic support for this project has been provided by CONACyT grant G32526-T.

BIBLIOGRAPHY

ARZATE J. A., O. DELGADO-RODRIGUEZ, J. O. CAMPOS-ENRIQUEZ and J. URRUTIA-FUCUGAUCHI, 2000. Electric structure of the Chicxulub impact basin along two magnetotelluric profiles. Submitted to Can. J. Earth Sci.

BERDICHEVSKY, M. N. and V. I. DMITRIV, 1976. Basic principles of interpretation of magnetotelluric sounding curves. A. Adam (Editor). Geoel. Geoth. Studies. KAPG Geophysical Monograph. Akademiai Kiado. Budapest, 165-221.

CAGNIARD, L., 1953. Basic theory of the magnetotelluric method of geophysical prospecting. *Geophysics, 18,* 605-635.

CAMPOS-ENRIQUEZ, J. O., J. A. ARZATE, J. URRUTIA-FUCUGAUCHI and O. DELGADO-RODRIGUEZ, 1997. The subsurface structure of the Chicxulub crater (Yucatan, Mexico): Preliminary results of a magnetotelluric study. *The Leading Edge. 16*, 1774-1777.

CHEN, J., H. W. DOSSO and M. INGHAM, 1990 Electromagnetic induction in New Zealand: Analogue model and field results. *Phys. Earth Plant. Inter., 62*, 257-270.

CONSTABLE, S. C., R. L. PARKER and C. G. CONSTABLE, 1987. Occam's inversion: A practical algorithm for generating smooth models from electromagnetic sounding data. *Geophysics, 52*, 289-300.

DELGADO-RODRIGUEZ, O., J.O. CAMPOS-ENRIQUEZ, J. URRUTIA-FUCUGAUCHI and J. A. ARZATE, 2000. Occam and Bostick 1-D inversion of magnetotelluric soundings in the Chicxulub impact crater, Yucatan, Mexico. Submitted to Geofís. Int.

DOSSO, H. W. and Z. W. MENG, 1992. The coast effect response in geomagnetic field measurements. *Phys. Earth Plant. Inter., 70*, 39-56.

CONNORS, M., A. R. HILDEBRAND, M. PILKINGTON, C. ORTIZ-ALEMAN, R. E. CHAVEZ, J. URRUTIA-FUCUGAUCHI, E. GRANIEL-CASTRO, A. CAMARA-ZI, J. VASQUEZ and J. F. HALPENNY, 1996. Yucatan karst features and the size of Chicxulub crater. *Geophys. J. Int., 27*, F11-F14.

ESPINDOLA, J. M., M. MENA, M. DE LA FUENTE and J. O. CAMPOS-ENRIQUEZ, 1995. A model of the Chicxulub impact structure (Yucatan, Mexico) based on its gravity and magnetic signatures. *Phys. Earth Plant. Inter., 92*, 271-278.

GOLDBERG, S. and Y. ROTSTEIN, 1982. A simple form of presentation of magnetotelluric data using the Bostick transform. *Geophys. Prosp., 30*, 211-216.

HEBERT, D., J. A. WRIGTH, H. W. DOSSO and W. NIENABER, 1983. Comparison of analogue model and field station results for the Newfoundland region. *J. Geom. Geoelectr., 35*, 673-682.

HILDEBRAND, A. R., G. T. PENFIELD, D. A. KRING, M. PILKINGTON, A. CAMARGO, S. JACOBSEN and W. BOYTON, 1991. Chicxulub crater: A possible Cretaceous/Tertiary boundary impact crater on the Yucatan Peninsula, Mexico. *Geology, 19*, 867-871.

HILDEBRAND, A. R., M. PILKINGTON, C. ORTIZ-ALEMAN, R. E. CHAVEZ, J. URRUTIA-FUCUGAUCHI, M. CONNORS, E. GRANIEL, A. CAMARA, J. F. HALPENNY and D. NIEHAUS, 1998. Mapping Chicxulub crater structure with gravity and seismic reflection data. *In:* Grady, M.M. *et al.* (Eds.),

Meteorites: Flux with Time and Impact Effects, Geol. Soc., London, Sp. Publ., *140*, 155-176.

KELLET, R. L., F. E. M. LILLEY and A. WHITE, 1991. A two-dimensional interpretation of the geomagnetic coast effect of southeast Australia, observed on land and sea-floor. *Tectonophysics, 192*, 367-382.

MENG, Z., H. W. DOSSO, L. K. LAW, F. W. JONES and V. RAMASWAMY, 1979. An analogue model study of E.M. induction in the North China-Korea coast region. *Phys. Earth Planet. Inter., 60*, 25-39.

NIENABER, W., H. W. DOSSO, L. K. LAW, F. W. JONES and V. RAMASWAMY, 1979. An analogue model study of electromagnetic induction in the Vancouver Island region. *J. Geomag. Geoelectr., 31*, 115-132.

MORGAN, J., M. WARNER and CHICXULUB WORKING GROUP, 1997. Size and morphology of the Chicxulub impact crater. *Nature, 390*, 472-476.

PARKINSON, W. D., 1959. Directions of rapid geomagnetic fluctuations. *Geophys. J. R. Astron. Soc., 2*, 1-14.

PARK, S. R., 1985. Distortion of magnetotelluric sounding curves by three-dimensional structures. *Geophysics, 50*, 785-797.

PENFIELD, G. T. and Z. A. CAMARGO,1981. Definition of a major igneous zone in the central Yucatan platform with aeromagnetics and gravity. 51st Ann. Internat. Mtg. SEG, Abstract, 37.

PILKINGTON, M., A. R. HILDEBRAND and C. ORTIZ-ALEMAN, 1994. Gravity and magnetic field modeling and structure of the Chicxulub crater, Mexico. *J. Geophys. Res. 99*, 147-162.

SHARPTON, V. L., K. BURKE, A. CAMARGO, S. A. HALL, D. SCOTT-LEE, L. MARIN, G. SUAREZ, J. M. QUEZADA, P. D. SPUDIS and J. URRUTIA-FUCUGAUCHI, 1993. Chicxulub multiring impact basin: Size and other characteristics derived from gravity analysis. *Science, 261*, 1564-1567.

URRUTIA-FUCUGAUCHI, J., L. MARIN and A. TREJO-GARCIA, 1996. UNAM scientific drilling program of Chicxulub impact structure. Evidence for a 300 kilometer crater diameter. *Geophys. Res. Lett., 23*, 1565-1568.

VOZOFF, K., 1972. The magnetotelluric method in the exploration of sedimentary basins. *Geophysics, 37*, 98-141.

Omar Delgado-Rodríguez[1,2], Jaime Urrutia-Fucugauchi[1], Jorge A. Arzate[3] and Oscar Campos-Enríquez[1]

[1] Departamento de Geomagnetismo y Exploración, Instituto de Geofísica, Universidad Nacional Autónoma de México, Coyoacán, 04510 México, D.F., México
email: omar@quetzalcoatl.igeofcu.unam.mx
[2] Instituto de Geofísica y Astronomía. Ministerio de Ciencia, Tecnología y Medio Ambiente, Calle 212, No. 2906, La Lisa, Ciudad de la Habana, Cuba
[3] Unidad de Investigación en Ciencias de la Tierra, UNAM-Campus Juriquilla, 76230 Juriquilla, Qro., México